Chemical Engineering Journal 102 (2004) 171–184

Chemical Engineering Journal

www.elsevier.com/locate/cej

Composite membranes for hydrophobic pervaporation: study with the toluene–water system

S.V. Satyanarayana, A. Sharma, P.K. Bhattacharya*

Department of Chemical Engineering, Indian Institute of Technology Kanpur, Kanpur 208016, India

Accepted 3 May 2004

Abstract

Composite membranes were utilized for hydrophobic pervaporation. Experiments were carried out with the toluene–water system using composite membranes (PERVAP® 1060 and PERVAP® 1070) and the results were analysed. The chosen membranes were characterised using a positron annihilations technique to measure free volume. In order to study solute–membrane interactions, the diffusion coefficient of toluene with in the membrane and Flory–Huggins interaction parameters (surface thermodynamic approach through contact angle measurement) were estimated. Influences of operating conditions (downstream pressure, feed toluene concentration, feed temperature) were observed on pervaporate fluxes (toluene and water) and pervaporate concentration of toluene.

The selectivities of the chosen composite membranes were observed to be lower compared to known values of selectivities for dense PDMS membrane, suggesting the role played by the support layer in this regard. Individual fluxes of toluene and water increase with increase in feed temperature; however, fluxes decrease with increase in downstream pressure. Further, pervaporate concentration of toluene increases with increase in feed concentration. Similar expected trends were observed; but in case of PERVAP® 1070, the toluene flux attained a plateau with increase in feed toluene concentration. Such a trend confirmed the presence of an extra component (possibly zeolites) in the skin layer of PERVAP® 1070. A simple resistance-in-series model, along with the solution-diffusion model were employed for mathematical analysis of the results. Model predictions with experimental values showed close agreements for the PERVAP® 1060 membrane while deviations were observed for the PERVAP® 1070 membrane.

Keywords: Pervaporation; Toluene/water; Composite membranes; Contact angle; Positron annihilations; Mathematical analysis

1. Introduction

Water contaminated with volatile organic compounds is encountered in several chemical industries, groundwater and site remediation applications. Conventional technologies such as air stripping and adsorption with activated carbon do not always provide a complete and economic solution for some of these waste water applications. In recent years, pervaporation [1–3] using hydrophobic membrane has been observed to be promising and potentially a suitable remediation method for such applications. Pervaporation is a membrane technology utilizing a dense non-porous homogeneous polymeric film. The liquid feed solution is in contact with the membrane at the upstream side, which is at atmospheric pressure. The liquid solute selectively dissolves and diffuses in the membrane and is removed as vapour at the downstream side. The pervaporation is carried out by maintaining the downstream pressure, lower than the saturation pressure of the permeating liquid solute at that temperature. Usually a higher vacuum is maintained to carry out the operation.

Several applications of pervaporation to organic contaminants laden wastewater are reported in the literature [4,5]. Interestingly, most of these studies were conducted with single organic component systems, such as toluene in water, etc. Certainly, this has a merit; as such an attempt may help to understand better the mechanism of pervaporation. Since toluene is less soluble in water, such studies were carried out within the soluble region (less than 500 ppm). Different types of membranes (e.g., polydimethyl siloxane (PDMS), ethylene-propylene diene terpolymers (EPDM), etc.) were utilized [5,6] for toluene–water separation. Most of the studies on the toluene–water system have been carried out using dense membranes. Practically, no work is available using composite membrane which makes the present study interesting. Particularly, these two different types of membranes (dense membranes versus thin-layer interfacial polymerization over a porous structure for composite membrane) may control solute transport behaviour

* Corresponding author. Tel.: +91 512 2597093; fax: +91 512 2590104.
E-mail address: pkbhatta@iitk.ac.in (P.K. Bhattacharya).

1385-8947/$ – see front matter © 2004 Elsevier B.V. All rights reserved.
doi:10.1016/j.cej.2004.05.005

Nomenclature

a	activity
b	constant in the free volume ($1/m^3$)
c	molar concentration ($kmol/m^3$)
C	volumetric concentration (m^3/m^3)
D	diffusivity (m^2/s)
E	activation energy (J/kg)
f	free volume fraction in the skin layer
H	Henry's law constant (mmHg)
I_3	intensity in Eq. (22)
J	volumetric flux (m^3/m^2 s)
k_L	molar concentration-based mass transfer coefficient (m/s)
K_L	molar concentration-based overall mass transfer coefficient (m/s)
k_m	mass transfer coefficient in the membrane ($kmol/m^2$ mmHg s)
k_x	mole fraction-based mass transfer coefficient ($kmol/m^2$ s)
K_x	mole fraction-based overall mass transfer coefficient ($kmol/m^2$ s)
l	thickness of membrane (m)
N	molar flux ($kmol/m^2$ s)
p	downstream pressure (mmHg)
$\bar{p}$	average permeability in the membrane (m kmol/m^2 mmHg s)
$\bar{P}$	overall average permeability (m kmol/m^2 mmHg s)
p^0	saturation pressure (mmHg)
P60	PERVAP®1060
P70	PERVAP®1070
r	spherical free volume size (m)
R	universal gas constant (J/kmol K)
Δr	electron layer thickness (m)
t	time (s)
T	absolute temperature (K)
v_p	velocity of the fluid (m/s)
V_F	free volume of skin layer (m^3)
x	liquid-phase mole fraction
y	vapour-phase mole fraction
z	axial coordinate

Greek symbols

α	overall selectivity
β	individual selectivity
γ	activity coefficient
δ	boundary layer thickness (m)
λ	constant in Eq. (24)
μ	chemical potential
ρ	molar density (kmol s/m^3)
τ_3	lifetime in Eq. (22) (s)

Subscripts

0	reference state
1	solution side
2	water side
b	bulk
i	organic component
m	inside membrane
s	surface
w	water

Superscripts

act	actual
F	feed side
int	intrinsic
P	permeate side
Perm	permeation
vap	vaporization

in different ways. Therefore, the objective of this study is to understand the role of the composite nature of the membrane along with its porous support layer for toluene–water separation using PERVAP (Sulzer Tech, Germany) membranes. Accordingly, two such PERVAP membranes (1060 and 1070) were chosen, based on the measurements of contact angles of the feed components, for the purpose of the present study. PERVAP membranes, however, have also been used for other systems, such as methanol–MTBE [7], aroma compounds–water [8], butanol–water [9], etc.

Transport through a dense membrane has been described [10]. Resistance-in-series model [11] has been widely used. Further, simplified equations for such a model were introduced for different transport steps during VOC removal. Its simplistic approach, with the film theory to account for the mass transfer limitations in the boundary layer, has attracted many researchers. The present work also adopts resistance-in-series model along with the solution-diffusion model. However, the model requires the solubility of the component in the membrane but it is practically impossible to estimate the amount of sorption in commercial membranes (because of the difficulty to discriminate between the active layer and the porous support layer), as stated by Gonzalez and Uribe [7]. Hence, in order to estimate the amount of sorption, another objective of this study is to estimate the Flory–Huggins interaction parameter using the relationship between surface tension and solubility.

2. Theory

2.1. Mass transport

The transport mechanism of trace organics in an aqueous solution through a dense hydrophobic membrane by pervaporation may be described by five consecutive steps, as shown in Fig. 1:

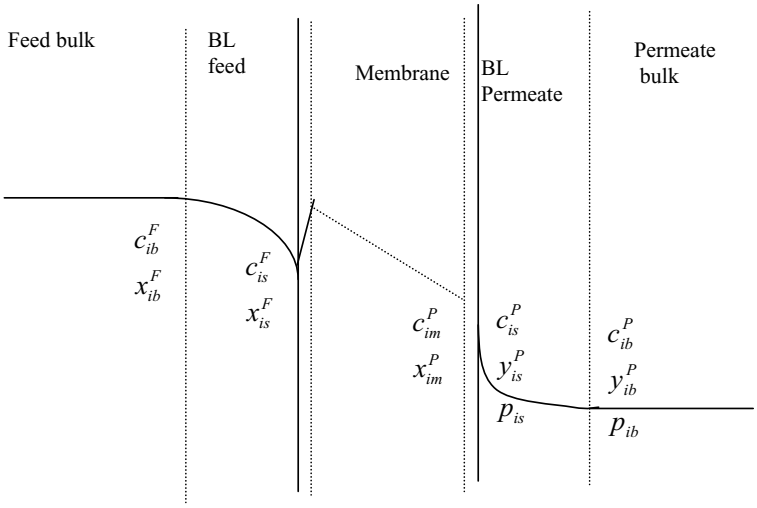

Fig. 1. Mass transport steps during pervaporation process.

(i) Diffusion of a penetrant from the bulk of the feed through the boundary layer to the feed membrane interface.
(ii) Dissolution of the penetrant into the membrane.
(iii) Diffusion of penetrant through the membrane to the downstream side.
(iv) Desorption of the penetrant as vapour at the permeate side.
(v) Diffusion of penetrant from the vapour–membrane interface through the boundary layer to the vapour permeate bulk.

2.1.1. Mass transport in the boundary layer

A mass balance of component i, in the feed side boundary layer over membrane surface may be obtained at steady state. The sum of convective and diffusive flux towards the membrane surface is equal to the permeate flux of component i [5]. The obtained equation may thus be integrated with appropriate boundary conditions to obtain a mass transfer coefficient, $k_{L,i}$ ($= D_i^F/\delta$) assuming the stagnant film theory to be valid (denoting D for diffusivity and δ for boundary layer thickness):

$$k_{L,i} = \frac{v_P}{\ln((\alpha_{iw}^{act} - \alpha_{iw}^{int}\alpha_{iw}^{act})/(\alpha_{iw}^{int} - \alpha_{iw}^{int}\alpha_{iw}^{act}))} \quad (1)$$

where, v_p ($=N/\rho$) is the velocity of the fluid perpendicular to the membrane surface and N, ρ denotes molar flux, molar density, respectively. Further, the following separation factors, α, of pervaporation process are calculated based on concentrations of feed and permeate:

$$\alpha_{iw}^{act} = \frac{y_{ib}^P/y_{wb}^P}{x_{ib}^F/x_{wb}^F} \approx \frac{y_{ib}^P}{x_{ib}^F} \quad (y_{wb}^P = x_{wb}^F \cong 1.0) \quad (2)$$

$$\alpha_{iw}^{int} = \frac{y_{is}^P/y_{ws}^P}{x_{is}^F/x_{ws}^F} \approx \frac{y_{ib}^P}{x_{is}^F} \quad (y_{ws}^P = x_{ws}^F \cong 1.0 \text{ and } y_{is}^P = y_{ib}^P) \quad (3)$$

where x, y are liquid and vapour-phase mole fractions. Superscripts F, P, act, and int signify feed, permeate, actual and intrinsic properties, respectively. Subscripts b, s, w signify bulk, surface and water, respectively. The ideal or intrinsic separation factor α_{iw}^{int} is calculated based on the membrane interface concentrations of the components. Mole fractions of water in feed and permeate were assumed to be one (both feed and permeate were very dilute solutions).

2.1.2. Influence of concentration and downstream pressure on flux and separation factor

The mass transfer across the boundary layer on the feed side can be described by

$$N_i = k_{L,i}(c_{ib}^F - c_{is}^F) = k_{x,i}(x_{ib}^F - x_{is}^F) \quad (4)$$

where c is the molar concentration. The mass transfer across the membrane is described by Fick's law with activity, a being the driving force. Further, the activity inside the membrane can be described as the product of the activity coefficient, γ_i, and the mole fraction, x_i. At low concentrations, activity coefficient inside the membrane may be considered to be constant. Therefore, volumetric flux, J, or molar flux, N, may be written as

$$J_i = -C_i D_i \frac{d \ln a_i}{dz} = -\frac{C_i D_i}{x_i}\frac{dx_i}{dz} \quad \text{or} \quad N_i = -\rho D_i \frac{dx_i}{dz} \quad (5)$$

where C is the volumetric concentration (m^3/m^3). Integration of Eq. (5) across the membrane (considering the concentrations in the membrane) leads to Eq. (6) as

$$N_i = -\rho \frac{\bar{D}_i}{l}(x_{im}^P - x_{im}^F) \quad (6)$$

where $\bar{D}_i$ and l are the mean diffusion coefficient through the membrane and membrane thickness, respectively. The solution-diffusion model assumes that equilibrium is at both sides of membrane interfaces, including the sorption and the desorption steps. At equilibrium, chemical potential, μ, at the membrane interface is equal to the chemical potential inside the membrane. This condition is same for both sides (feed and permeate). Thus, activities also are related in the same way for constant pressure in the membrane:

$$\mu_{is}^{F} = \mu_{im}^{F} \Rightarrow a_{is}^{F} = a_{im}^{F} \tag{7}$$

$$\mu_{is}^{P} = \mu_{im}^{P} \Rightarrow a_{is}^{P} = a_{im}^{P} \tag{8}$$

Further, assuming that the vapours in the permeate side behave as ideal gas

$$a_{is}^{F} = \gamma_{is}^{F} x_{is}^{F} \quad \text{and} \quad a_{is}^{P} = \frac{p y_{is}^{P}}{p_i^0} = \frac{p y_{ib}^{P}}{p_i^0} \tag{9}$$

where p and p^0 are partial and saturation vapour pressures, respectively. Eq. (9) was obtained assuming the ratio of fugacity coefficients as well as the *Poynting* factor to be equal to 1. Hence, the concentrations inside the membrane for both sides can be obtained by combining Eqs. (7)–(9). Therefore

$$x_{im}^{F} = \frac{\gamma_{is}^{F}}{\gamma_{im}^{F}} x_{is}^{F} \quad \text{and} \quad x_{im}^{P} = \frac{p}{p_i^0} \frac{y_{ib}^{P}}{\gamma_{im}^{P}} \tag{10}$$

The molar flux is then obtained by inserting Eq. (10) into Eq. (6); accordingly,

$$N_i = \frac{\rho \bar{D}_i}{l \gamma_{im}^{F} p_i^0} (\gamma_{is}^{F} x_{is}^{F} p_i^0 - p y_{ib}^{P}) = k_{m,i} (x_{is}^{F} H_i - p_{ib}) \tag{11}$$

where H_i ($= p_i^0 \gamma_{is}^{F} = p_i^0 \gamma_{ib}^{F}$) and $k_{m,i}$ ($= \bar{p}_{m,i}/l$) are Henry's law constant and mass transfer coefficient, respectively. Further, $\bar{p}$ denotes average permeability in the membrane. Eq. (11) was obtained assuming the activity coefficient throughout membrane to be constant. Analogous to gas separation, it is convenient to define an overall pervaporation flux in terms of vapour pressure difference as

$$N_i = \frac{\bar{P}_i}{l} (p_i^0 \gamma_{ib}^{F} x_{ib}^{F} - p_{ib}) = K_{x,i} \left(x_{ib}^{F} - \frac{p_{ib}}{H_i} \right) \tag{12}$$

where $\bar{P}$ and K ($K_{x,i} = \bar{P}_i H_i / l$) denote overall average permeability and overall mass transfer coefficient, respectively. At steady state, the flux through each layer is same, and therefore, the overall mass transfer coefficient may be related to film mass transfer coefficients:

$$\frac{1}{K_{x,i}} = \frac{1}{k_{x,i}} + \frac{1}{H_i k_{m,i}} \tag{13}$$

Further, the molar concentration-based overall mass transfer coefficient and mole fraction-based mass transfer coefficient are related by $K_{L,i} = K_{x,i}/\rho$. In the case of downstream pressure tending to zero ($p \to 0$), Eq. (12) becomes

$$N_i = K_{x,i} x_{ib}^{F} \tag{14}$$

For two-component systems (organics and water), the water flux was also analysed in the similar way. However, for pervaporation of dilute organic solutions, the boundary layer mass transport resistance for water is assumed to be negligible. So, the water flux can be expressed as

$$N_w = \frac{\bar{P}_w}{l} (p_w^0 \gamma_w^{F} x_w^{F} - p_{wb}) \tag{15}$$

For dilute aqueous solution, γ_w^{F} and x_w^{F} may be assumed to be equal to 1. If the downstream pressure is negligible, Eq. (15) can then be simplified as

$$N_w = \frac{\bar{P}_w p_w^0}{l} \tag{16}$$

Influence of downstream pressure on separation factor can be obtained by rearranging Eqs. (12) and (15) as

$$\frac{y_{ib}^{P}}{y_{wb}^{P}} = \frac{\bar{P}_i}{\bar{P}_w} \frac{H_i}{p_w^0} \left[\frac{(x_{ib}^{F} - p y_{ib}^{P}/H_i)}{(1 - p y_{wb}^{P}/p_w^0)} \right] \tag{17}$$

Let

$$\beta^{perm} = \frac{\bar{P}_i}{\bar{P}_w} \quad \text{and} \quad \beta^{vap} = \frac{H_i}{p_w^0} \tag{18}$$

Therefore, Eq. (18) can now be written as

$$\frac{y_{ib}^{P}}{y_{wb}^{P}} = \beta^{perm} \beta^{vap} \left[\frac{(x_{ib}^{F} - p y_{ib}^{P}/H_i)}{(1 - p y_{wb}^{P}/p_w^0)} \right] \tag{19}$$

For dilute organic solutions, then Eq. (19) can be further written as

$$\frac{1}{\alpha_{iw}^{act}} = \frac{1}{\alpha_{0,iw}^{act}} + \left(\frac{\beta^{perm} - 1}{\alpha_{0,iw}^{act}} \right) \frac{p}{p_w^0} \tag{20}$$

where separation factor $\alpha_{0,iw}^{act}$ ($= \beta^{perm} \beta^{vap}$) is at zero downstream pressure. Thus, the increase or decrease of separation factor with downstream pressure depends on the value of β^{perm}.

2.1.3. Influence of temperature on flux

The temperature dependence on flux at constant upstream and downstream conditions was considered as per *Arrhenius*-type [16] relationship:

$$N_i = N_{0,i} \exp \left(-\frac{\Delta E_i}{RT} \right) \tag{21}$$

where ΔE is the activation energy. Similar relationship may also be written for water flux.

3. Experimental

3.1. Materials

Toluene (99% purity) was obtained from Ranbaxy, India. Double-distilled water was used to prepare the feed solutions. Membranes (PERVAP®1060 and PERVAP®1070) were obtained from Sulzer Chemtech, Germany. These are composite membranes consisting of a porous support (70–100 μm) on top of a polymer fleece (non-woven fabric of thickness of 100 μm). On top of the porous support is a very thin but dense (0.5–2 μm) separating layer (proprietary polymer).

3.2. Analysis

The toluene concentration in both the feed and the permeate samples were analysed using UV spectroscopy (Shimadzu, Japan) at a wavelength of 261.5 nm. The results were also cross checked using a gas chromatograph (Nuchon, India) equipped with FID. Puropack-Q was used as the reference column and chromosorb as the main column. The oven, injector, and detector temperatures were set at 120, 170, and 180 °C, respectively. Benzene was used as the internal standard. Nitrogen was used as carrier gas. Retention time for benzene was 1.94 min and that for toluene was 2.46 min.

3.3. Positron annihilation lifetime (PAL) measurements

The PAL measurements were carried out using a fast–fast system having a resolution of 300 ps (FWHM for the ^{60}Co prompt γ-rays, under ^{22}Na window settings). Details of PAL measurements are already presented in an earlier work [12]. The following expression was used to relate *ortho*-positronium (*o*-Ps) pick-off lifetime, τ_3, and free volume radius, r [13]:

$$\tau_3 = \frac{1}{2}\left[1 - \frac{r}{r+\Delta r} + \left(\frac{1}{2\pi}\right)\sin\left(\frac{2\pi r}{r+\Delta r}\right)\right]^{-1} \quad (22)$$

Further, the fractional free volume f may be estimated from empirical relationship [13]:

$$f = bV_F I_3 \quad (23)$$

where V_F and I_3 are the free volume of the sphere and intensity of *o*-Ps. The scaling factor b is obtained from variation of free volume with temperature. However, in the absence of such data, it may be typically assigned [14] a value of 1.0 nm^{-3}.

3.4. Diffusion coefficient

The diffusion coefficient of organic component within the membrane was estimated in a specially fabricated experimental cell made of glass. The design of cell and estimation procedure was adapted from Barnes [15]. Two stirred chambers (filled volume = 400 ml) were separated by a membrane with an effective surface area of 36.78 cm^2. The chambers are held together using Perspex flanges. Feed solution was filled in one chamber and the other chamber was filled with distilled water. Heating arrangements were provided for both the chambers in order to estimate diffusion coefficients under varied temperatures. The temperatures of the solutions were measured using a PT-100 thermocouple. Constant temperature was maintained using a proportional controller. Samples were taken at regular intervals from the water chamber and analysed for toluene content. The following equation [16] was used to estimate the diffusion coefficient:

$$C_2(t) = \tfrac{1}{2}C_1(0)[1 - e^{-2\lambda Dt/l^2}] \quad (24)$$

where $C_1(0)$ and $C_2(t)$ are the initial concentration of toluene (solution side) and concentration at any time, t at side 2 (pure water side), respectively. Further, λ is the constant.

3.5. Contact angle measurements

Equilibrium contact angles of toluene and 'probe liquids' in a saturated environment on the chosen membranes were measured by sessile drop method using a Goniometer (Rame-Hart, Inc. Imaging System, USA). Details of contact angle measurements are already presented in an earlier work [12]. The variation of measured contact angles are ±2° with PERVAP®1060 membrane and ±8° with PERVAP®1070 membrane. The larger variation of contact angle with PERVAP®1070 may be due to the presence of more than one component.

3.6. Pervaporation experimental setup

The experimental setup, designed and developed in our laboratory, was used for the pervaporation measurements, shown in Fig. 2. The pervaporation test cell of around 400 ml was made of glass, having specially designed flanges to lodge the membrane with an effective membrane area of 40.7 cm^2. The membrane was kept on highly porous stainless steel support with the shiny polymeric layer facing the feed solution. Toluene was dissolved in water by providing sufficient agitation to prepare the binary solution. A three-neck round-bottom flask was used to circulate feed solution to the test cell. The flask was filled with 1 l of the feed solution. The solution and feed cell was heated separately to desired temperature. The temperature was controlled through a PID controller device (Fuji, Japan). Any loss of feed as vapour, formed due to heating, was recovered by placing a condenser on top of the PV test cell.

The feed solution was circulated to the upstream side of the membrane through a long capillary channel, using a peristaltic pump, while retentate was sent back to the flask. Sufficient feed flow rate was maintained (around 300 ml/min). The temperature of the feed solution in the cell was measured using a PT-100 thermocouple with an accuracy of ±0.2 °C.

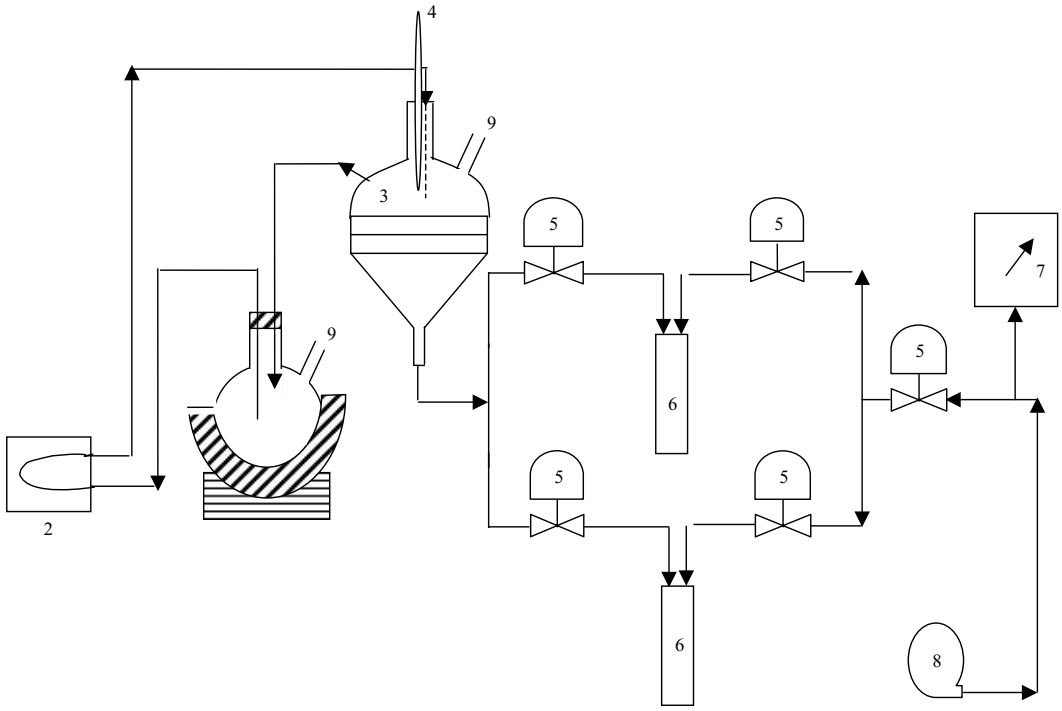

1 —Preheating Cell, 2—Peristaltic pump, 3—Pervaporation cell, 4—thermocouple, 5—Needle valves, 6—Liquid traps placed in Dewar flask, 7—McLeod Gauge, Pirani gauge, Capillary column in parallel mode 8—Vacuum Pump, 9—Condenser

Fig. 2. Schematic diagram of experimental setup for pervaporation.

The membrane upstream side was kept at atmospheric pressure and the downstream side was maintained under vacuum through the use of a pump (Vacuum Techniques, Bangalore). Total downstream pressure was measured by a Meclod/Pirani/Capillary column and was regulated with an air inlet using stainless steel micro-needle valve, located between the condensers and the vacuum pump.

The condenser system consisted of two traps that can be used alternately, allowing the permeated pervaporate stream to be sampled continuously without interruption of the operation. The permeated vapours were condensed in the trap by keeping it in a Dewar flask, filled with liquid nitrogen. The frozen permeate was collected within a specified time interval. The cold traps were brought to room temperature prior to measurement of their weight using a five decimal balance (Afcoset, India) to determine the mass flux.

Experiments were conducted to observe the influence of independent variables: temperature (40, 50, 60 °C), downstream pressure (24, 1333, 2000 Pa) and feed toluene concentration (50, 100, 200 ppm) on dependent variables: mass flux and extent of separation (toluene concentration in permeate). The flux values and the toluene concentration were recorded in the permeate as a function of time; however, in the present work, values were obtained after around 4 h and are reported when almost no change of values was observed in the measurement. To minimize measurement errors, an average of the three separate consecutive readings were taken after the system attained steady state. The average error in the total permeation mass flux was estimated around ±1% and that for the toluene concentration was around ±5%.

Further, in order to record permeate concentration under negligible concentration polarization effect, permeate samples were taken during initial period of experimentation (just around 15 min or so). This was done to observe and estimate intrinsic separation factor where the surface concentration would be almost equal to feed bulk concentration.

4. Results and discussion

4.1. Composite membrane characterization

4.1.1. Positron annihilations technique

The positron lifetime spectroscopy analysis was made for varieties of dense and composite membranes in order to obtain primarily free volume parameters. The findings as well as salient results have been presented in the form of a separate communication [17]. In this paper, however, results pertaining to P60 and P70 are utilized and presented in Table 1. The results show that the lifetime (τ_3) is the same for both the membranes. This indicates the polymer may be the same for both the membranes. The extra lifetime (τ_4) for P70 is matched with the lifetime for zeolites [18]. Hence, the difference in the pervaporation results may be attributed due to the presence of zeolite. Further, the obtained free volume parameters are agreement with theoretical values [19].

Table 1
Free volume parameters and skin layer thickness of P60 and P70

Membrane	τ_3 (ns)	I_3 (%)	r (nm)	V_f (nm^3)	F	l^a ($\times 10^{-6}$ m)
P60	2.3 ± 0.02	9.4 ± 0.2	0.311	0.126	0.012	41.7
P70	2.32 ± 0.28; τ_4: 4.53 ± 0.48	10.6 ± 1.5; I_4: 5.1 ± 2.0	0.307, 0.45	0.128, 0.385	0.013, 0.049	16.5

[a] Average thickness of skin layer: estimated through scanning electron microscopy.

4.2. Solute–membrane interactions

4.2.1. Diffusion coefficient

As per the Eq. (24), plots of time t versus $\log[1 - 2C_2(t)/C_1(0)]$ were drawn at different feed concentrations and temperature for both P60 and P70 membranes. The value of the diffusion coefficient, D, was estimated using the slopes of these lines, along with the respective estimates of λ and l. The value of λ (=effective free volume/liquid volume) was estimated by taking the effective free volume as the product of effective surface area of the membrane, membrane thickness (Table 1) and free volume fraction of the membrane (Table 1). The obtained values of diffusivities as functions of temperature and feed concentration are shown in Fig. 3. The larger values of diffusion coefficients indicate suitability of the rubbery polymers for pervaporation of toluene.

Further, diffusion coefficient values were found to be 3–100 times lower compared to the value of diffusion coefficient of chloroform (for 100 ppm solution of chloroform) for dense PDMS membrane [16]. Even though, the pervaporation selectivity for toluene/water and chloroform/water are in the same range for dense PDMS membrane [11,16], the smaller diffusion coefficients for the toluene, in the present case, may be because of the presence of support layer of the composite membrane. Apart from this, few other observations from Fig. 3 are: (i) diffusion coefficient for toluene is more in P60 compared P70 membrane, (ii) diffusivity of toluene is decreasing with increasing feed concentration for P70 while it was found to be independent for P60 membrane and (iii) diffusion coefficient is increasing with increasing temperature for both the membranes but the increase is more for P60 compared P70.

4.2.2. Estimation of Flory–Huggins interaction parameter

The basic theory behind the estimation of the Flory–Huggins interaction parameter is presented in an earlier work [12]. The surface tension values of probe liquids at 20 °C are taken from literature [20]. Measured values of contact angles are reported in Table 2 which also includes the calculated values of surface tensions. The obtained surface tension values suggest the mono-polar nature of the chosen membranes. The Flory–Huggins interaction parameter between toluene and membranes taking minimum contactable surface area for the toluene [21] as 0.44 nm^2 were calculated and reported in Table 2. The interaction parameter of toluene with P60 is 0.2462 (close to the value known for PDMS [10] membrane) and for P70 is 0.2556. It is

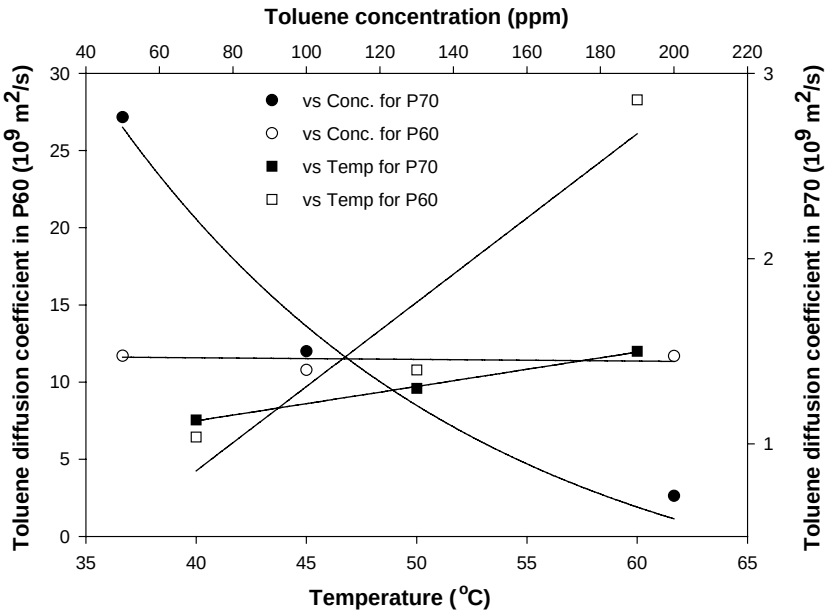

Fig. 3. Variation of diffusion coefficient of toluene with feed toluene concentration and temperature.

Table 2
Contact angles, surface tensions of membranes and interaction parameter

Parameters	P60	P70
Contact angle of water (°)	93.8	84.8
Contact angle of ethylene glycol (°)	78.8	76.6
Contact angle of diodo-methane (°)	74.8	75.2
Lifshitz–vander Waals surface tension (mJ/m^2)	20.21	20.01
Electron acceptor surface tension (mJ/m^2)	0.026	0.003
Electron donor surface tension (mJ/m^2)	5.819	13.44
Surface tension (mJ/m^2)	20.98	20.43
Interfacial tension between toluene and membrane	1.13	1.15
Interaction parameter of toluene with membrane	0.2462	0.2501
Interfacial tension between water and membrane	26.12	13.85
Interaction parameter of water with membrane	1.0332	0.5478

known [22] that low values of interaction parameters (less than 0.5) suggest the dissolution of the skin layer with pure toluene. There are lot of speculations with regard to contactable surface area of water molecules. The average contactable surface area of single water molecule [23] is roughly 0.08 nm^2. Using this value, the interaction parameter for water was estimated and also reported in Table 2. The smaller value of interaction parameter between water and P70 suggests high sorption and low selectivity compared to P60.

4.3. Estimation of mass transfer coefficient in the boundary layer

As mentioned in the experimental section, permeate samples collected for a shorter run (around 15 min) were analysed and the results are reported in Table 3. Further, pseudo-steady-state results are also reported in Table 3. Due to the large variation of selectivity with feed concentration for P70 membrane (elaborate discussion in the following sections), the shorter run results are reported only at 105 ppm.

From the values of intrinsic and actual separation factors, the mass transfer coefficient in the boundary layer was calculated using Eq. (1). The average value of mass transfer coefficient in the boundary layer was estimated to be 2.35×10^{-6} m/s for P60 membrane and 1.00×10^{-6} m/s for P70. The obtained mass transfer coefficient is comparable to the value (6.06×10^{-6} m/s for PEBA at 25 °C and 170 rpm) obtained by Raghunath and Hwang [5]. However, in principle, the boundary layer mass transfer coefficient is independent of membrane material but certainly a function of concentration, albeit a weak function. Selectivity of toluene was found to be lower for P70 compared to P60 membrane. Therefore, concentration gradient in the boundary layer was observed to be small in the case of P70 and hence lower boundary layer mass transfer coefficient. Such results were also reported by Nijhuis et al. [24] for the separation of toluene through PDMS and EPDM membranes. This was explained due to deviations during extrapolation of their results. Further, the overall flux for shorter runs was found to be slightly higher than that obtained at pseudo-steady-state conditions for P60 membrane. This may be due to the fact that initially the toluene concentration at the membrane surface is greater. Because of this, membrane swelling (interaction coefficient: 0.2462) and flux are observed to be higher. Similar observations can also be made for the slight increase of overall flux with increase in feed toluene concentration. However, the membrane swelling, in case of P70, may be less and hence the observed difference in flux between shorter and steady-state runs is small.

Against expectations, it is to be noted from Table 3 that both selectivities (intrinsic and actual) for the membranes are much lower compared to pure PDMS dense membrane [11]. Such lower values of selectivities are attributed because of the composite nature of the membrane (very thin skin layer on support layer). For elastomeric polymers, the organic flux is independent of membrane thickness [24] and water flux is dependent. Therefore, water flux was observed to be higher. Further, low values of intrinsic selectivity may be because of the role played by the support layer (diffusion path length, pressure loss and permeate condensation). These values depend on the support structure (porosity, pore size) and material property. Feng and Huang [25] reported on the specific role of the support layer in terms of the separation of acetic acid–water mixtures using silicone-based membranes. The homogeneous silicone-polycarbonate co-polymer membrane was found to be acetic acid selective, while silicone-polycarbonate co-polymer membrane on a micro-porous support structure was slightly water selective. Likewise, several such studies [26,27] have reported the importance of support layer during pervaporation separation.

Quantitative estimation of diffusion path length and pressure loss in the support layer may be carried out, but rigorous calculations are required [27]. Hence, only the permeate

Table 3
Experimental data for estimation of mass transfer coefficient (fluxes, permeate concentrations and separation factor)

Membrane	Feed concentration (ppm)	Short-run flux ($\times 10^{-6}$ kmol/m^2 s)	Short-run permeate concentration (ppm)	α_{iw}^{int}	Steady-state flux ($\times 10^{-6}$ kmol/m^2 s)	Steady-state permeate concentration (ppm)	α_{iw}^{act}
P60	45	5.811	1805.7	40.12	5.597	728.1	16.18
	100	5.980	3821.1	38.21	5.633	1307.2	13.07
	200	6.333	7020.6	35.10	5.878	2880.0	14.40
P70	105	3.631	2992.8	28.50	3.608	1090.5	10.38

condensation in the pores of P70 support layer was considered for the present work. An average pore size of support layer was assumed to be 25 nm which is similar to ultrafiltration membranes [28]. Further, the non-woven fabric of the composite membrane was carefully removed and the contact angles of water and toluene on the porous support were measured. The average contact angle for water was found to be $127 \pm 4^{\circ}$ and for toluene it was 0°. These values were used to estimate the saturation vapour pressure in the porous support layer using Kelvin's equation [29].

Because of the support layer, the equilibrium vapour pressure for water in the pore thus increased from 92.51 to 94.63 mm of Hg, while toluene vapour pressure decreased from 92.1 to 84.6 mm of Hg. This suggests toluene condensation in the support layer and provides reason for lower selectivity, as compared to dense membrane. The change in vapour pressure depends strongly on the pore size of support layer. Further, regardless of the radius of the pore of support layer, water vapour pressure increases while toluene vapour pressure decreases.

4.4. Effect of operating parameters

4.4.1. Influence of toluene feed concentration

Fig. 4 shows the effect of feed toluene concentration on toluene flux at 50 °C. Linear relationships were obtained for both the membranes (for the range of feed toluene concentrations, chosen for the work). The toluene flux increases with increase in toluene concentration. This is because of the increase in solubility and driving force with increase in concentration and the trend verifies Eq. (14). However, although the experimental values for P70 fall in a straight line, the line does not pass through the origin. This may be due to the fact that, in the developed model, the diffusion coefficient and the activity coefficient of the permeant are assumed to be independent of concentration. In general, they are concentration-dependent [30] and hence simple relationship in the form Eq. (14) was obtained (detailed discussion follows in Section 4.5 regarding this aspect). Baker et al. [31] reported similar results for pervaporation of dilute aqueous solutions of toluene through silicone rubber membranes. Neglecting the initial behaviour pattern of toluene flux, a linear fit of the experimental points was obtained and as per Eq. (14), the overall mass transfer coefficients, $K_{x,\mathrm{i}}$, were estimated from the slopes of the fitted lines. The obtained values are divided with the molar density of the solution to estimate overall mass transfer coefficients, $K_{\mathrm{L},\mathrm{i}}$ (Table 4). For the same flow rate, overall mass transfer coefficient for P60 is higher than the one obtained for P70. Further, an attempt was made to fit P70 results using exponential and hyperbolic relations and the results are found to be comparable (Fig. 4). This non-linearity may be due to the exponential variation of diffusivity or *Langmuir* sorption with concentration or may be both. As observed from diffusion experiments (Section 4.2.1) the diffusion coefficient of toluene in the membrane is a function of feed concentration. It is to be mentioned here that Ji and Sikadar [32] reviewed the experimental results as well as the models for pervaporation of various mixtures in adsorbent-filled membranes, and according to them, sorption may be dual-sorption.

According to Eq. (16), the water flux is independent of feed toluene concentration at higher downstream vacuum. The experimental values for water flux at high downstream vacuum and at 50 °C are also shown in Fig. 4. Almost constant water flux is observed. The deviation may be due to coupling (because of swelling) which is not accounted in the developed model. Ji et al. [11] have reported constant water flux with increase in feed organic concentration for the permeation of dilute aqueous solutions of toluene, methylene chloride and trichloroethane through PDMS and PEBA

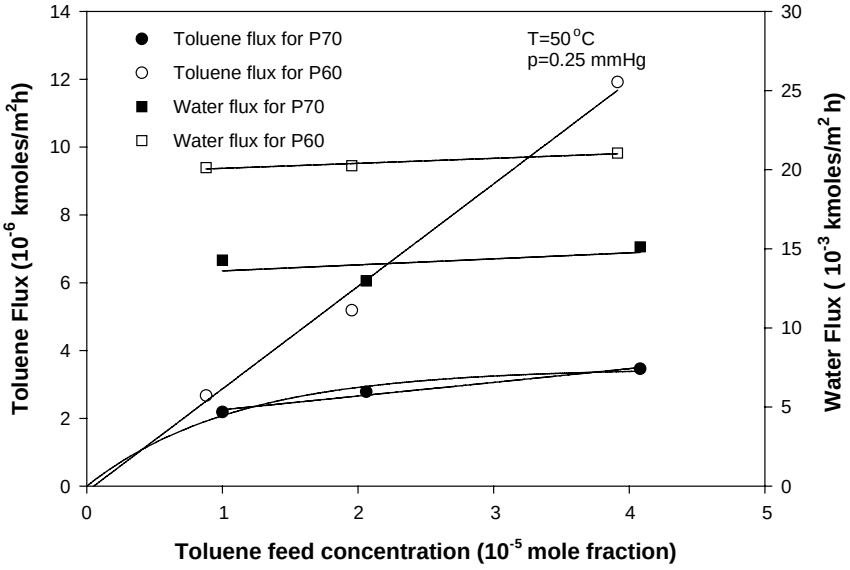

Fig. 4. Influence of feed toluene concentration on individual fluxes.

Table 4
Estimated values of overall mass transfer coefficient, water permeability and activation energy under set experimental conditions

Parameters	P60	P70	Conditions
$k_{L,i}$ ($\times 10^{-6}$ m/s)	2.35	1.00	$T = 50\,^{\circ}C$, $p \approx 0$
$K_{L,i}$ ($\times 10^{-6}$ m/s)	1.51	0.38	$T = 50\,^{\circ}C$, $p \approx 0$
P_w ($\times 10^{-10}$ m kmol/m^2 s mmHg)	2.48	0.64	$T = 50\,^{\circ}C$, $p \approx 0$
$K_{L,i}$ ($\times 10^{-6}$ m/s)	1.35	0.72	$T = 50\,^{\circ}C$, $p > 0$, $x_{ib}^{F} = 1.95 \times 10^{-5}$
H_i (mmHg)	251.75	257.94	$T = 50\,^{\circ}C$, $p > 0$, $x_{ib}^{F} = 1.95 \times 10^{-5}$
$k_{m,i}$ ($\times 10^{-6}$ kmol/m^2 mmHg s)	0.70	0.54	$T = 50\,^{\circ}C$, $p > 0$, $x_{ib}^{F} = 1.95 \times 10^{-5}$
$\bar{p}_i$ ($\times 10^{-11}$ m kmol/m^2 mmHg s)	2.93	0.89	$T = 50\,^{\circ}C$, $p > 0$, $x_{ib}^{F} = 1.95 \times 10^{-5}$
ΔE_i ($\times 10^{3}$ kJ/g)	1.82	3.91	$p \approx 0$, $x_{ib}^{F} = 1.95 \times 10^{-5}$
ΔE_w ($\times 10^{3}$ kJ/g)	0.69	0.78	$p \approx 0$, $x_{ib}^{F} = 1.95 \times 10^{-5}$

membranes. However, Meuleman et al. [6] have reported increase of water flux with increase in toluene concentration through EPDM membrane. Hence, water permeabilities for both the membranes were estimated which are reported in Table 4. The water permeability for P70 was observed to be lower than that for P60.

4.4.2. Effect of downstream pressure

According to Eq. (12), for constant feed concentration, a plot of N_i versus p_{ib} should be a straight line with an intercept of $K_{x,i}x_{ib}^{F}$ and slope of $-K_{x,i}/H_i$. The experimental values of toluene flux against downstream partial pressure of toluene are shown in Fig. 5. Straight lines are obtained in the pressure range of 0.16–28 mmHg. Overall mass transfer coefficients were estimated from the intercepts (after dividing with molar density of the solution) and are reported in Table 4. These values were compared with the values obtained for feed concentration variation. Therefore, it is observed that the mass transfer coefficients values are comparable for the P60 membrane. However, the difference is larger for the case of P70 membrane. One can expect higher values of overall mass transfer coefficients with concentration variation (at high vacuum) compared to pressure variation because of the existence of vapour-phase resistance. However, the present case contrasts with this. As mentioned in Section 4.4.1, toluene flux plateaus with concentration; hence, the average concentration-based overall mass transfer coefficient was found to be smaller than that of downstream pressure-based mass transfer coefficient. This suggests that the vapour-phase mass transfer resistance is negligible in the range of chosen downstream pressures. Further, Henry's law constant was estimated (from the slope) and the values are reported in Table 4. With only small differences, the values were found to be same for both the membranes as well as being comparable to literature values [11,33,34]. The mass transfer coefficient in the membrane was also calculated (using mass transfer coefficients in the boundary layer) and the values are reported in Table 4. Fig. 5 also shows the linear variation of water flux with downstream pressure which is in agreement with Eq. (15).

Fig. 6 depicts the effect of downstream pressure on separation factor. According to Eq. (20), the reciprocal of separation factor increases with increase in downstream pressure (for β^{perm} greater than 1). Brun et al. [35] have

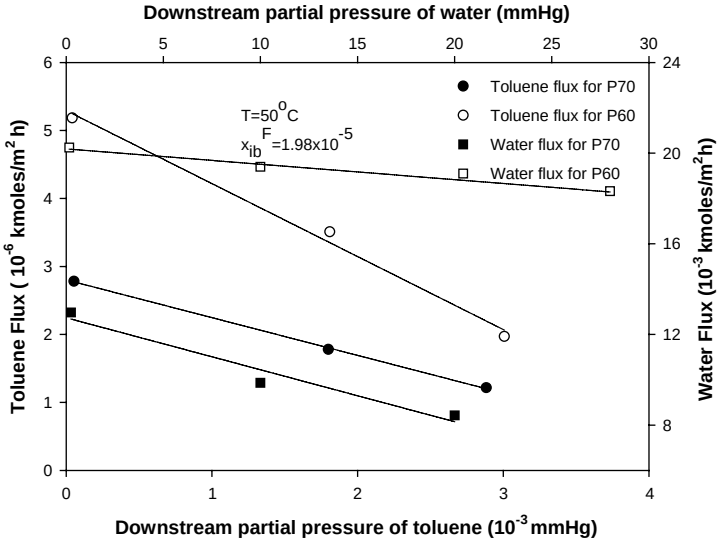

Fig. 5. Influence of downstream partial pressures on individual fluxes.

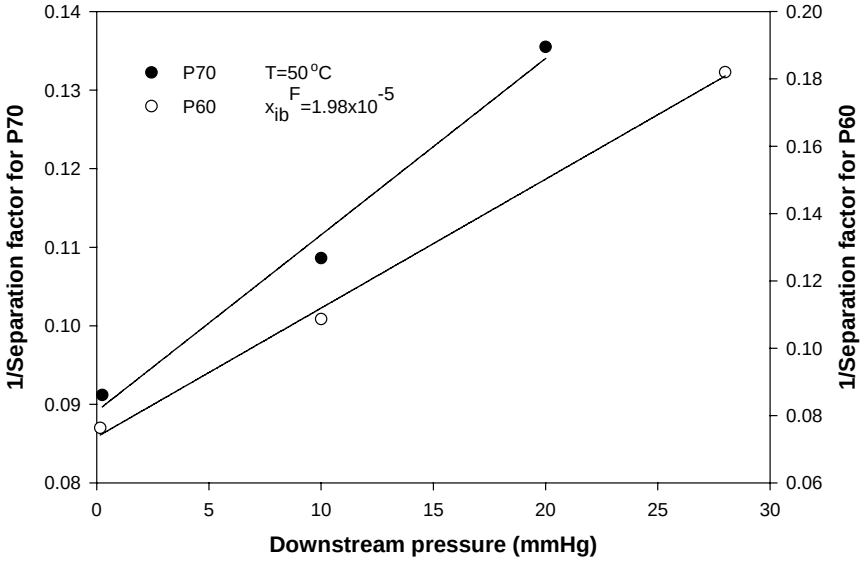

Fig. 6. Influence of downstream pressure on separation factor.

reported similar results for the separation of dilute solutions of benzene and chloroform using NBR and SBR membranes. Reverse trends have also been reported [11] using other polymeric membranes. In an interesting article Ten and Field [36] classified the systems into four classes, according to range of downstream pressures. As per their classification, the present system falls under class '*A*'. Accordingly, there is a sharp decrease in permeate concentration as permeate pressure increases (from absolute vacuum); the present work indeed shows such a case.

Further, it may interesting to observe from Fig. 6 that the variation of selectivity (in terms of slope) with pressure is more for P60 compared to P70. This may be because of the drop of pressure in the support layer. Pressure drop either for viscous flow (Knudsen number < 0.01) or for molecular flow (Knudsen number > 10) in the support layer is proportional to total flux [37,38]. The total flux obtained for P60 is higher and hence higher pressure drop. Increase in pressure drop reduces toluene flux and hence selectivity.

4.4.3. *Effect of temperature*

Arrhenius type of temperature dependency of permeate flux was studied and is shown in Fig. 7. Overall activation energy values for permeation of toluene and water (as per Eq. (21)) were estimated and are reported in Table 4. Even

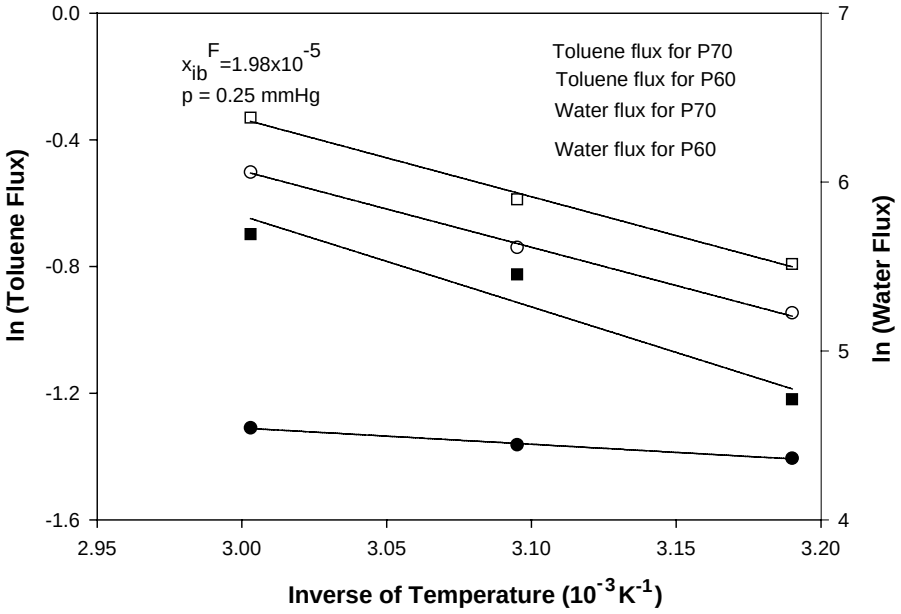

Fig. 7. Arrhenius plot: influence of feed solution temperature on individual fluxes.

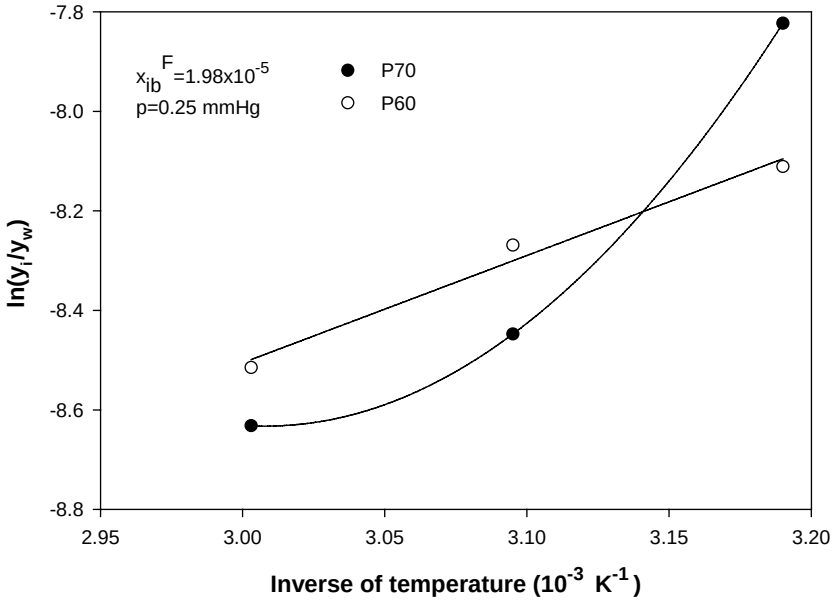

Fig. 8. Relationship between ratio of toluene to water (pervaporate) concentrations and reciprocal of temperature.

though, both water and toluene (Fig. 7) flux increase with increase in temperature, but the ratios of permeate concentration of toluene to water decrease with increase in temperature (Fig. 8). Increased water permeability at higher temperatures compared to toluene may be the explanation for the observed behaviour. Further, the increased water permeability may be because of either increase of solubility or diffusivity or may be both. Incidentally, the data fitting with P70 was found to be non-linear which is at variance with Eq. (21). Consistent to earlier observations, the trend is expected for the said filled membrane.

The presence of increased water fraction in the permeate, obviously, lowers the permeate concentration, resulting in decrease of separator factor. Further, the values of activation energies suggest faster permeation for water instead of toluene having higher activation energy (Table 4). Since the membrane is more selective to toluene than water, these two opposite characteristics lower the net permeation of toluene and thus selectivity gets lowered. Further, comparing Eqs. (14) and (16) and taking ratios of these two fluxes at negligible downstream pressure, the selectivity (pervaporate concentration ratio) simply becomes the ratios of saturation pressures of the two components. Knowing the rate of change of vapour pressure of toluene, being lower than water with increase in temperature [39,40], and the selectivity obviously decreases with increase in temperature. Therefore, if pervaporation process is carried out at lower temperature, higher selectivity may be achieved, but at the expense of the toluene production rate.

4.5. Performance of membranes: a comparison

Positron annihilations results confirmed the presence of two components in the skin layer of P70 membrane. Apart from the PDMS, silicalite zeolites may be the second component. Silicalite zeolites are known to have straight and zigzag channels connected via intersections. This may have caused differences in the results observed for the two membranes (Figs. 4–8). The overall flux and the toluene flux for the P60 membrane were observed to be higher than for the P70 membrane. Similar such low values of overall flux reported for zeolite-filled membranes are available [41–43]. This limitation on flux may be ascribed to the molecular sieving properties of the zeolites. The simulation results of adsorption of high organics (hexane) through silicalite showed the occurrence of capillary condensation of the organic components and formation of kink or step in adsorption isotherm [44]. Similarly, since toluene is the higher molecular weight molecule, capillary condensation of toluene may take place which may take longer time for withdrawal. Therefore, the P70 membrane provided lower toluene flux than P60. However, Goethaert et al. [45] observed much higher chlorinated hydrocarbon fluxes in the zeolite-filled membranes compared to unfilled membranes. Further, water and overall flux reduced to less than half to that of unfilled membrane. The toluene is a bigger molecule (molecular size ~0.6 nm) [33] compared to zeolite (0.49 nm). In addition, lower interaction between these two (toluene and zeolite) may be the reason for lower organic flux.

As mentioned earlier, the linear concentration profile obtained for P70 (Fig. 4) did not pass through the origin. This may be because at low concentration of toluene (50 ppm), the molecules move freely in the channels and at high concentration (200 ppm) the channels get saturated with the permeating molecules, preventing the free movement of molecules in the channels. Therefore, toluene flux attains plateau with increasing concentration.

Further, it may be stated that at low temperature, the toluene selectivity in the P70 membrane is higher compared to the P60. This may be because of the absence of kink formation in the adsorption isotherm at lower temperatures [46] compared to the presence of kink formation at higher temperatures [47].

5. Conclusions

The membranes selected for this study were characterised using the positron annihilation technique. The base polymers of skin layer for both membranes were found to be the same; however, the results for the P70 membrane showed the presence of an extra component (possibly zeolites). Diffusion coefficients of solute within the membrane as well as the solubilities were estimated in order to study the solute–membrane interactions. Toluene diffusivity within the membrane was observed to be independent of feed concentration for the P60 while it decreased with increase in feed concentration for the P70 membrane.

During hydrophobic pervaporation, lower values of intrinsic and actual selectivities for composite membranes, compared to dense membranes, suggested that an important role is played by the support layer. In the case of P70, toluene flux plateaus with increase in feed concentration which confirms the presence of an extra component in the skin layer.

The pervaporation experimental results were mathematically analysed with the application of Henry's law and with the use of concentration-independent diffusion coefficients. The results for the P60 membrane adhered to such a model, whereas the same were not observed to be valid for the P70 membrane. Therefore, a simple resistance in series model may not be sufficient enough for filled membranes.

Experimental data and results may be considered to be useful for the selection of support layer for better application of composite membrane. This may necessitate simulation and optimization between the geometry and physical properties of the support layer.

Acknowledgements

One of the authors (PKB) thankfully acknowledges the funding received from Indo-French Centre for Promotion of Advanced Research (IFCPAR) in partial support to this work.

References

[1] I. Blume, J.G. Wijmans, R. Baker, The separation of dissolved organics from water by pervaporation, J. Membr. Sci. 49 (1990) 253–286.
[2] P. Sampranpioon, R. Jiraratananon, D. Vttapap, X. Feng, R.Y.M. Huang, Pervaporation separation of ethyl butyrate and isopropanal with PEBA membranes, J. Membr. Sci. 173 (2000) 53–59.
[3] C. Viswanathan, B. Basu, J.C. Mora, Separation of volatile organic compounds by pervaporation for a binary compound combination: trichloroethylene and 1,1,1-trichloroethane, Ind. Eng. Chem. Res. 34 (1995) 3956–3962.
[4] C. Lipsi, P. Cote, The use of pervaporation for the removal organic contaminants from water, Environ. Prog. 9 (1990) 254–261.
[5] B. Raghunath, S.-T. Hwang, Effect of boundary layer mass transfer resistance in the pervaporation of dilute organics, J. Membr. Sci. 65 (1992) 147–161.
[6] E.E.B. Meuleman, J. Willemsen, M.H.V. Mulder, H. Strathaman, EPDM as a selective membrane material in pervaporation, J. Membr. Sci. 188 (2001) 235–249.
[7] B. Gonzalez, I.O. Uribe, Mathematical modeling of the pervaporative separation of methanol-methyl tert-butyl ether mixtures, Ind. Eng. Chem. Res. 40 (2001) 1720–1731.
[8] A. Baudot, I. Souchon, M. Marin, Total permeate pressure influence on the selectivity of pervaporation of aroma compounds, J. Membr. Sci. 158 (1999) 167–185.
[9] A. Baudot, I. Souchon, M. Marin, Dehydration of water/t-butanol by pervaporation: comparative study of commercially available polymeric, J. Membr. Sci. 197 (2002) 309–319.
[10] E.E.B. Meuleman, B. Bosch, M.H.V. Mulder, H. Strathmann, Modelling of liquid/liquid separation by pervaporation: toluene from water, AIChE J. 45 (1999) 2153–2160.
[11] W. Ji, S.K. Sikadar, S.T. Hwang, Modeling of multicomponent pervaporation for removal of volatile organic compounds from water, J. Membr. Sci. 93 (1994) 1–19.
[12] A. Sharma, S.P. Thampi, S.V. Suggala, P.K. Bhattacharya, Pervaporation from a dense membrane: roles of permeant–membrane interactions, Kelvin effect and membrane swelling, Langmuir, 20 (2004) 4708.
[13] S.J. Tao, Positronium annihilation in molecular substances, J. Chem. Phys. 56 (1972) 5499.
[14] S. Weinhold, G.M. Stack, M.R. Tant, A.J. Hill, Effect of copolymer composition on free volume and gas permeability in poly(ethylene terephthalate)-poly(1,4-cyclohexylenedimethylene terephthalate) copolyesters, Eur. Polym. J. 32 (1996) 843–849.
[15] C. Barnes, Diffusion through a membrane, Physics 5 (1934) 4.
[16] Y.M. Lee, D. Bourgeois, G. Belfort, Sorption, diffusion and pervaporation of organics in polymer membranes, J. Membr. Sci. 44 (1989) 161–181.
[17] S.V. Satyanarayana, V.S. Subrahmanyam, H.C. Verma, A. Sharma, P.K. Bhattacharya, Positron annihilation study of pervaporation dense membranes, J. Membr. Sci., submitted for publication.
[18] Y.C. Jean, Characterizing free volumes and holes in polymers by positron annihilation spectroscopy, in: Proceedings of the NATO Advanced Research Workshop on Advances with Positron Spectroscopy of Solids and Surfaces, Varenna, Italy, 16–17 July 1993.
[19] L.H. Sperling, Introduction to Physical Polymer Science, Wiley, New York, 1986.
[20] C.J. Van Oss, Interfacial Forces in Aqueous Media, Marcel Dekkar, New York, 1994.
[21] C.J. Van Oss, R.F. Giese, R.J. Good, The zero time dynamic interfacial tension, J. Disper. Sci. Technol. 23 (4) (2002) 455–464.
[22] M.H.V. Mulder, in: R.Y.M. Huang (Ed.), Thermodynamic Principles of Pervaporation, Pervaporation Membrane Separation Processes, Elsevier, Amsterdam, 1991, pp. 225–251.
[23] D. Eisenberg, W. Kauzmann, The Structure and Property of Water, Oxford University Press, Oxford, 1969, pp. 164–165.
[24] H. Nijhuis, M.H.V. Mulder, C.A. Smolders, Removal of trace organics from aqueous solutions: effect of membrane thickness, J. Membr. Sci. 61 (1991) 99–111.
[25] X. Feng, R.Y.M. Huang, Separation of isopropanol from water by pervaporation using silicone based membranes, J. Membr. Sci. 74 (1992) 171–181.
[26] J. Börjesson, H.O.E. Karlsson, G. Trägårdha, Pervaporation of a model apple juice aroma solution: comparison of membrane performance, J. Membr. Sci. 119 (1996) 229–239.

[27] F. Lipnizki, J. Olsson, P. Wu, A. Weis, G. Trägårdha, R.W. Field, Hydrophobic pervaporation: influence of the support layer of composite membranes on the mass transfer, Sep. Sci. Technol. 37 (8) (2002) 1747–1770.
[28] S. Singh, K.C. Khulbe, T. Matsuura, P. Ramamurthy, Membrane characterization by solute transport and atomic force microscopy, J. Membr. Sci. 142 (1998) 111–127.
[29] R.J. Hunter, Foundations of Colloidal Science, vol. 1, Clarendon press, Oxford, 1987.
[30] J. Olsson, G. Trägårdha, Pervaporation of volatile organic compounds from water. I. Influence of permeate pressure on selectivity, J. Membr. Sci. 187 (2001) 23–37.
[31] R.W. Baker, J.G. Wijmans, A.L. Athayde, R. Daniels, J.H. Ly, M. Le, The effect of concentration polarization on the separation of volatile organic compounds from water by pervaporation, J. Membr. Sci. 137 (1997) 159–172.
[32] W. Ji, S.K. Sikadar, Pervaporation using adsorbent-filled membranes, Ind. Eng. Chem. Res. 35 (1996) 1124–1132.
[33] D.T. Leighton, J.M. Cao, Distribution coefficients of chlorinated hydrocarbons in dilute air–water systems for ground water contamination applications, J. Chem. Eng. Data 26 (1981) 382.
[34] R.C. Reid, J.M. Prausnitz, T.K. Sherwood, The Properties of Gases and Liquids, McGraw-Hill, New York, 1997.
[35] J.P. Brun, L. Larchet, R. Merlet, G. Bulvestre, Sorption and pervaporation of dilute aqueous solutions of organic compounds through polymer membranes, J. Membr. Sci. 25 (1985) 55–100.
[36] P.K. Ten, R.W. Field, Organophilic pervaporation: an engineering science analysis of component transport and the classification to behaviour with reference to the effect of permeate pressure, Chem. Eng. Sci. 55 (2000) 1425–1445.
[37] R.E. Treybal, Mass-Transfer Operations, 3rd ed., McGraw-Hill, New York, 1986.
[38] M.H.V. Mulder, Basic Principles of Membrane Technology, Kluwer Academic Publishers, Dordrecht, The Netherlands, 1991.
[39] R.H. Perry, D. Green, Perry's Chemical Engineers' Hand Book, 6th ed., Mc-Graw Hill, New York, 1984.
[40] D.M. Himmelblau, Basic Principles and Calculations in Chemical Engineering, Prentice Hall of India, New Delhi, 1995.
[41] I.F.J. Vankelecom, J.D. Kinderen, B.M. Dewitte, J.B. Uytterhoven, Incorporation of hydrophobic porous fillers in PDMS membranes for use in pervaporation, J. Phys. Chem. B 101 (1997) 5182–5185.
[42] T. Lamer, A. Voilley, Influence of different parameters on the pervaporation of aroma compounds, in: Proceedings of the Fifth International Conference on Pervaporation Process in the Chemical Industry, Heidelberg, Germany, 11–15 March 1991.
[43] M. Jia, K.V. Peinemann, R.D. Behling, Molecular sieving effect of zeolite-filled silicone rubber membranes in gas permeation, J. Membr. Sci. 57 (1991) 289–292.
[44] B.M. Smit, T.L.M. Maeson, Commensurate 'freezing' of alkanes in the channels of a zeolite, Nature 374 (1995) 42–44.
[45] S. Goethaert, C. Dotremont, M. Kuijpers, M. Michiels, C. Vandecasteele, Coupling phenomena in the removal of chlorinated hydrocarbons by means of pervaporation, J. Membr. Sci. 78 (1993) 135–145.
[46] U. Lohse, H. Thamm, M. Noack, B. Fahike, J. Inclusion Phenom. 5 (1987) 307–313.
[47] R.E. Richard, L.V.C. Rees, Sorption and packing of *n*-alkane molecules in ZSM-5, Langmuir 3 (1987) 335–340.